Cross Calibration of SeaWiFS and MODIS Using On-Orbit Observations of the Moon

Robert E. Eplee, Jr.,[1,*] Jun-Qiang Sun,[2] Gerhard Meister,[3] Frederick S. Patt,[1] Xiaoxiong Xiong,[3] and Charles R. McClain[3]

[1]*Science Applications International Corporation, 4600 Powdermill Road, Suite 400, Beltsville, Maryland 20705, USA*

[2]*Sigma Space Corporation, 4801 Forbes Boulevard, Lanham, Maryland 20706, USA*

[3]*Hydrospheric and Biospheric Sciences Laboratory, Code 614, NASA Goddard Space Flight Center, Greenbelt, Maryland 20771, USA*

[*]*Corresponding author: Robert.E.Eplee@nasa.gov*

Observations of the Moon provide a primary technique for the on-orbit cross calibration of Earth remote sensing instruments. Monthly lunar observations are major components of the on-orbit calibration strategies of SeaWiFS and MODIS. SeaWiFS has collected more than 132 low phase angle and 59 high phase angle lunar observations over 12 years, Terra MODIS has collected more than 82 scheduled and 297 unscheduled lunar observations over 9 years, and Aqua MODIS has collected more than 61 scheduled and 171 unscheduled lunar observations over 7 years. The NASA Ocean Biology Processing Group's Calibration and Validation Team and the NASA MODIS Characterization Support Team use the USGS RObotic Lunar Observatory (ROLO) photometric model of the Moon to compare these time series of lunar observations over time and varying observing geometries. The cross calibration results show that Terra MODIS and Aqua MODIS agree, band-to-band, at the 1-3% level, while SeaWiFS and either MODIS instrument agree at the 3-8% level. The combined uncertainties of these comparisons are 1.3% for Terra and Aqua MODIS, 1.4% for SeaWiFS and Terra MODIS, and 1.3% for SeaWiFS and Aqua MODIS. Any residual phase dependence in the ROLO model, based on these observations, is less than 1.7% over the phase angle range of $-80°$ to $-6°$ and $+5°$ to $+82°$. The lunar cross calibration of SeaWiFS, Terra MODIS, and Aqua MODIS is consistent with the vicarious calibration of ocean color products for these instruments, with the vicarious gains mitigating the calibration biases for the ocean color bands. © 2010 Optical Society of America

OCIS codes: 280.0280, 010.1690, 120.0280, 120.5630, 280.4780, 280.4991

1. Introduction

Observations of the Moon provide a unique way of cross calibrating two or more remote sensing satellite instruments on orbit. This paper presents the results of the cross calibration of SeaWiFS, Terra MODIS, and Aqua MODIS. The latest on-orbit calibrations derived for these instruments are applied to the lunar data to correct for radiometric drifts, thus allowing comparisons to be made with stable top-of-the-atmosphere (TOA) radiances. A comparison of lunar data analysis methodologies developed by the NASA Ocean Biology Processing Group's Calibration and Validation Team (OBPG CVT) and the NASA MODIS Characterization Support Team (MCST) to provide these on-orbit calibrations for SeaWiFS and MODIS has been reported previously [1,2] and is summarized below. The cross calibration presented here uses all 8 SeaWiFS bands and the MODIS reflective solar bands with wavelengths shorter than 900 nm that do not saturate on the Moon (bands 1-4 and 8-12). The SeaWiFS and MODIS bands being compared are shown in Table 1. MODIS bands 13-16 are discussed as part of the vicarious calibration validation later in this paper, so they are shown here despite their saturation on the Moon. The cross calibration results presented

here will compare the instrument calibrations first as a function of wavelength and then as a function of phase angle.

The cross calibration uses lunar data collected by all three instruments over their missions through April of 2009. A summary of the lunar observations is shown in Table 2. SeaWiFS has made 132 monthly lunar observations at a nominal phase angle of 7°, distributed before and after full phase; these observations are the primary on-orbit monitor of the radiometric response of SeaWiFS. It has also made an observation at a phase angle of $-27°$ during the EOS Lunar Cross Calibration Experiment [3] on 14 April 2003. To extend the phase angle range of the lunar observations, SeaWiFS has made 59 lunar observations distributed over nominal phase angles of $-45°$ to $-28°$, and $+28°$ to $+55°$. Terra MODIS has made 82 scheduled monthly lunar observations by rolling the spacecraft to a nominal phase angle of $+55°$, while Aqua MODIS has made 61 scheduled monthly observations by rolling the spacecraft to view the Moon at a nominal phase angle of $-55°$; these observations are the primary on-orbit monitors of the radiometric response for the two MODIS instruments at the angle of incidence (AOI) of the space view port on the scan mirror. There are also about thirty unscheduled lunar observations every year for both MODIS instruments, where the Moon is fully visible in the space view port for one or more orbits before or after the scheduled lunar observations. These unscheduled observations occurred over a range of phase angles because the spacecraft was not rolled to control the phase angle of the observations. Terra MODIS has obtained 297 observations over a phase angles of $+55°$ to $+82°$, while Aqua MODIS has obtained 171 observations at phase angles of $-54°$ to $-80°$. In addition, Terra MODIS made an observation at a phase of $-27°$ during the 14 April 2003 Lunar Cross Calibration Experiment. The end date for the cross calibration of April 2009 has been chosen because of operational issues with SeaWiFS spacecraft since that time and the subsequent low number of additional SeaWiFS lunar calibrations. Because of the large number of lunar observations involved in the comparisons, the lunar observations that have been obtained since April 2009 by the three instruments would not affect the outcome of the cross calibration.

The USGS RObotic Lunar Observatory (ROLO) photometric model of the Moon [4–6] is used to correct each instrument's lunar measurements for variations in the geometry of the observations, namely the changing Earth-Sun and Earth-Moon distances, and the phase and libration angles of the observations. The ROLO model also accounts for differences in the spectral bandpasses of the instruments. The use of residuals of the lunar observations from the ROLO model allows the instrument cross calibrations to be made over different time periods and phase angle ranges.

The ultimate goal of this cross calibration is to determine the calibration biases between the three instruments on orbit. There are several sources of uncertainty in the cross comparison that must be accounted for to achieve this goal. One source of uncertainty is the observational scatter in a single lunar observation; this uncertainty is mitigated by maximizing the number of observations that can be used for each comparison made in the cross calibration. A second source of uncertainty are the instrument-specific corrections for changes in instrument response with scan angle, denoted as RVS (response versus scan angle); these

corrections are applied to the Terra Lunar Cross Calibration Experiment observations and to all of the SeaWiFS observations. A third source of uncertainty are the differences in phase angles of the calibrations used in the comparisons; the primary lunar calibrations have been obtained at $-55°$ (Aqua MODIS), $-7°$ (SeaWiFS), $+7°$ (SeaWiFS), and $+55°$ (Terra MODIS). The residual phase dependence of the ROLO model given as 1% or less [6]; one of the goals of this study is to investigate the phase independence of the ROLO model using on-orbit data. We will discuss the impact that each of these sources of uncertainty has on the determination of the calibration biases between instruments. In the paper, we will provide background information on the SeaWiFS and MODIS lunar data and the geometric corrections provided by the ROLO model, then we will present the results of the cross calibration comparisons over wavelength and over phase angle.

2.   The Lunar Calibrations

For the cross calibration between SeaWFS and the MODIS instruments, each lunar data set has been calibrated with the latest radiometric calibration for that instrument to yield stable, TOA radiances for the comparisons. The lunar calibration time series for SeaWiFS or either MODIS, is given by [7]:

$$L_{Moon}(r,t,\lambda) \;=\; L_T(r,t,\lambda)\,K_{vg}(r,t,\lambda)\,K_{os}(r,t) \tag{1}$$

where:

r	$\equiv$	position relative to the Earth's center
t	$\equiv$	time of the observation
λ	$\equiv$	instrument band
L_T	$\equiv$	at-sensor radiance of the observation
K_{vg}	$\equiv$	corrections for viewing geometry
K_{os}	$\equiv$	oversampling correction.

The ROLO model is used to correct the lunar observations for viewing geometry (Sun/Moon distance, spacecraft/Moon distance, phase angle, libration angles); the geometry corrections are discussed further in the following section of the paper. The oversampling corrections are different for SeaWiFS and the two MODIS instruments because of the different techniques used to observe the Moon. The SeaWiFS and MODIS lunar calibration observations will be discussed in turn.

2.A.   SeaWiFS Observations

SeaWiFS observes the Moon on a monthly basis through its nadir view, which requires a spacecraft pitch maneuver. During a lunar calibration, the spacecraft attitude control system is set to open loop and spacecraft is pitched across the Moon, so SeaWiFS views the Moon near nadir through the same optical path as it views the Earth. The pitchrate across the Moon (in the along-track direction) is slower than the scan rate of the instrument, resulting in an oversampled image of the Moon. A typical Band 1 lunar image is shown in Fig. 1.

During the pitch maneuvers the spacecraft horizon sensors lose track of the Earth's horizon, so the pitchrate of the spacecraft is not known during the calibrations and varies from one calibration to the next. Consequently, the OBPG CVT computes the oversampling correction for a given calibration by dividing the actual size of the Moon, as seen from the spacecraft, by the apparent size of the Moon in the lunar image. At the same time, the observing geometry causes SeaWiFS to view the Moon at different scan angles from one calibration to the next; the variation in instrument response with scan angle is corrected by an RVS correction.

The size of the Moon in the lunar images is derived from the radiance profile across the Moon. The size of the lunar image is dependent on the angle between the along-track direction of the spacecraft field-of-view during the pitch maneuver and the rotational axis of the Moon, or the track angle of the observation. A spacecraft track that is not along the rotational axis of the Moon could intersect the lunar terminator rather than the edge of the Moon, yielding an underestimate of the actual size of the Moon in the lunar image.

A correction for this size underestimation is dependent on both the track angle and on the phase angle of the lunar image (which determines the location of the terminator) [7]. The correction of the image size due to the track angle and the phase angle is:

$$K_{track}(r,t) \; = \; \frac{\cos\alpha(r,t)}{\sqrt{1 \; - \; (1 \; + \; \cos\alpha(r,t))\,(1 \; - \; \cos\alpha(r,t))\,\cos^2\gamma(r,t)}} \tag{2}$$

where:

$\alpha \;\equiv\;$ phase angle

$\gamma \;\equiv\;$ track angle

The size of the Moon, corrected for the track angle, is:

$$Y_{Moon}(r,t) \; = \; \frac{2}{K_{track}(r,t) \; + \; 1} \, Y_{obs}(t) \tag{3}$$

where $Y_{obs} \;\equiv\;$ observed size of the Moon in fractional pixels. The track angle corrections for the low phase angle lunar calibration time series have values of 1.0–1.0034, with a mean of 1.0013 ± 0.0011. Since the track angle corrections are functions of phase angle, the high phase angle corrections have values of 1.0001–1.198, with a mean of 1.029 ± 0.037.

The oversampling correction for the SeaWiFS lunar images has the form:

$$K_{os}(r,t) \; = \; \frac{1}{\theta\,Y_{Moon}(r,t)} \, \frac{D_{Moon}}{R_{Inst-Moon}(r,t)} \tag{4}$$

where:

$R_{Inst-Moon} \;\equiv\;$ instrument – Moon distance

$D_{Moon} \;\equiv\;$ diameter of the Moon (3476.4 km)

$\theta \;\equiv\;$ instantaneous field of view SeaWiFS (1.5911 mrad)

This equation shows that the size of the oversampling correction for SeaWiFS is a strong function of the lunar phase angle. At high phase angles (and corresponding instrument scan angles) the image of the Moon in the SeaWiFS field of view rotates slightly with respect to the along-track direction, thus increasing the track-angle and making the determination

of the size of the lunar image more difficult; this image rotation increases the uncertainty in the oversampling correction. The oversampling correction time series for the SeaWiFS low phase angle lunar observations are shown in Fig. 2. The low phase angle corrections vary over a range of 0.203–0.302 with a mean value of 0.275 ± 0.012 while the high phase angle corrections vary over a range of 0.149–0.278 with a mean value of 0.216 ± 0.032. The plot and statistics for the corrections support the conclusion that the variations in the oversampling correction from calibration to calibration are the primary source of the scatter in the SeaWiFS lunar observations, particularly for high phase angles. This conclusion will be discussed further during as part of the calibration comparisons over wavelength. The primary cause of the variations in the oversampling correction are the variations in the pitchrate of the spacecraft across the Moon during the lunar calibration.

2.B. MODIS Observations

The MODIS reflective solar bands are calibrated primarily by the on-board calibrators, the solar diffuser and the solar diffuser stability monitor, which track the radiometric response of the instrument at the AOI of the diffuser on the scan mirror, 50.25°. MODIS also views the Moon approximately monthly through its space view port to monitor the instrument response at the AOI of the space view, 11.4°. The MODIS scheduled lunar observations usually require a spacecraft roll maneuver to keep the lunar phase angle within a small range. The difference in the response at the two AOIs represents the on-orbit change of the RVS of the MODIS scan mirror. A typical MODIS lunar calibration is shown on the left in Fig. 3. The spacecraft rolls so that the instrument views the Moon at a fixed phase angle through the space view port. Two successive scans across the Moon, one for each mirror side, are shown in Fig. 4 for the three spatial resolutions of 250m, 500m, and 1000m (these spatial resolutions are for Earth pixels at nadir, not lunar pixels). For analyses performed on a per band basis, MCST averages the integrated lunar radiances over the detectors in each band for multiple scans of the Moon, precluding the need of an oversampling correction. The analyses reported in this paper have taken this band-averaged approach to the lunar data. For analyses performed on a per detector basis, MCST produces a composite lunar image for each detector from the image sequence, as shown on the right in Fig. 3. These composite images of the Moon require an oversampling correction for subsequent analysis. The oversampling correction for MODIS is computed from the size of the scan in the along-track direction across the Moon and from the size of a pixel on the lunar surface [8].

The size of the scan is computed from the scan duration and the velocity of the track on the lunar surface:

$$DT_{Moon}(\rho, r, t) = \Delta T \, V_{track}(\rho, r, t) \tag{5}$$

where

$$
\begin{aligned}
V_{track} &\equiv \text{track velocity on the lunar surface} \\
\rho &\equiv \text{spacecraft roll angle} \\
\Delta T &\equiv \text{MODIS scan period (1.477 s)}
\end{aligned}
$$

The track velocity is computed from a projection of the spacecraft orbital velocity on the lunar surface:

$$V_{track}(\rho, r, t) = V_{orb}(r, t) \left(1 + \frac{R_{Inst-Moon}(r, t)}{R_{Inst-Earth}(r, t)} \sin(-\rho + \delta) - V_{proj}(r, t) \right) \quad (6)$$

where

$$
\begin{aligned}
R_{Inst-Earth} &\equiv \quad \text{Instrument-Earth distance} \\
V_{orb} &\equiv \quad \text{spacecraft orbital velocity} \\
\delta &\equiv \quad \text{offset angle of the spaceview port } (-8.425°) \\
V_{proj} &\equiv \quad \text{projection of the spacecraft velocity on the lunar surface}
\end{aligned}
$$

The projection of the spacecraft velocity on the lunar surface is:

$$V_{proj}(r, t) = \frac{\vec{V}_{orb}(r, t) \cdot \vec{V}_{Moon}(r, t)}{V_{orb}^2(r, t)} \quad (7)$$

where $V_{Moon} \equiv$ the orbital velocity of the Moon. The size of a pixel on the lunar surface given by:

$$P_{Moon}(r, t) = \theta \, R_{Inst-Moon}(r, t) \quad (8)$$

where $\theta \equiv$ instantaneous field of view MODIS (1.4179 mrad).

The oversampling correction for the MODIS composite lunar images has the form:

$$K_{os}(\rho, r, t) = \frac{DT_{Moon}(\rho, r, t)}{P_{Moon}(r, t)} = \frac{\Delta T \, V_{track}(\rho, r, t)}{\theta \, R_{Inst-Moon}(r, t)} \quad (9)$$

This equation shows that the size of the oversampling correction for MODIS is a strong function of the spacecraft roll angle. The oversampling correction time series for both sets of MODIS scheduled lunar calibrations are shown in Fig. 2. The corrections for Terra MODIS vary over a range of 0.171–0.548 with a mean value of 0.355 ± 0.094, while the corrections for Aqua MODIS vary over a range of 0.185–0.553 with a value mean of 0.369 ± 0.099. The plots and statistics for the corrections show that the behavior for the two instruments is comparable and the variations from calibration to calibration are larger than those observed for SeaWiFS. However, as has been pointed out earlier in this section, the MODIS oversampling corrections are only applied in analyses performed on a detector-by-detector basis. The lunar cross calibration results reported in this paper are based on MODIS band-averaged lunar radiances, so the variations in the oversampling corrections to not impact the SeaWiFS / Terra MODIS / Aqua MODIS comparisons reported here.

2.C. Validation of the Oversampling Corrections

The comparison of the SeaWiFS oversampling correction (Equation 4) with the MODIS oversampling correction (Equation 9) shows that the corrections for both SeaWiFS and MODIS are physically consistent:

$$K_{os}(r, t) = \frac{1}{\theta \, Y_{Moon}(r, t)} \frac{D_{Moon}}{R_{Inst-Moon}(r, t)} = \frac{\Delta T \, V_{track}(\rho, r, t)}{\theta \, R_{Inst-Moon}(r, t)} \quad (10)$$

This equation can be reduced to:

$$\frac{D_{Moon}}{Y_{Moon}(r,t)} = \Delta T \, V_{track}(\rho, r, t) \tag{11}$$

which is the size of the scan in the along-track direction across the Moon, determined from the lunar images plus observing geometry for SeaWiFS and from the spacecraft roll angle plus observing geometry for MODIS. This comparison validates these two approaches to computing oversampling corrections for the lunar observations.

3. Corrections for Viewing Geometry

The lunar irradiance observed by Earth-orbiting remote sensing instruments depends on the viewing geometry. The USGS has developed the ROLO photometric model of the Moon to provide the geometric corrections for lunar observations obtained by these instruments over the wavelength range of 300-2500 nm [4–6]. The model explicitly accounts for the effects of distances, phase, lunar libration, the opposition effect, and albedo variations of the lunar surface. The model uses relative spectral responses for each band of a given instrument to generate disk-integrated lunar irradiances as seen by those bands, thus taking into account the bandpass differences between the instruments. The ROLO model eliminates the requirement of simultaneous observations of the Moon for cross-calibration purposes.

The ROLO model requires as input the disk-integrated lunar irradiance for each band of the instrument in question (without any viewing geometry corrections applied), along with the time of the lunar observation and the three-dimensional location of the spacecraft at the time of the observation. The model predicts the disk-integrated albedo of the Moon and computes the solar irradiance for the specified band, then uses the time of the observation and the position of the spacecraft at that time to compute the viewing geometry of the observation. Finally, the model computes the lunar irradiance at the time and position of the Moon as seen by the instrument. The radiometric output of the model is the residual between the instrument measurement and the model prediction:

$$P(r, \lambda, t) = \frac{K_d(r,t)}{A_{Moon}(r, \lambda, t)} \frac{E_{Inst}(r, \lambda, t)}{E_{Sun}(\lambda)} - 1 \tag{12}$$

where:

$E_{Inst} \quad \equiv \quad$ lunar irradiance measured by the instrument.
$K_d \quad \equiv \quad$ Sun-Moon and Instrument-Moon distance corrections.
$A_{Moon} \quad \equiv \quad$ lunar albedo predicted by the model.
$E_{Sun} \quad \equiv \quad$ solar irradiance.

The distance corrections have the functional form of:

$$K_d(r,t) = \left(\frac{R_{Sun-Moon}(r,t)}{AU}\right)^2 \left(\frac{R_{Inst-Moon}(r,t)}{MLD}\right)^2 \tag{13}$$

where:

$$
\begin{aligned}
R_{Sun-Moon} &\equiv & \text{Sun – Moon distance} \\
\text{AU} &\equiv & \text{Astronomical Unit} \\
R_{Inst-Moon} &\equiv & \text{Instrument – Moon distance} \\
\text{MLD} &\equiv & \text{mean Earth – Moon distance} = 384401 \text{ km.}
\end{aligned}
$$

The predicted lunar albedo A_{Moon} is a function of the phase angle and libration angles of the observation and the instrument bandpasses. The phase functions of the Moon are a set of empirically-derived polynomials of the phase angle with additional terms arising from the opposition effect [4]. The phase functions at three wavelengths which span the wavelength range of the cross calibration analysis (412 nm, 555 nm, and 856 nm) are shown in Fig. 5.

The uncertainty in the absolute calibration of the ROLO model is $5-10\%$ [5]. The stability of the model output and the reliability for prediction of irradiance variation with geometry far exceeds the absolute accuracy. The ROLO model allows lunar observations to provide highly precise information about the relative change in radiometric performance of satellite instruments over time and about the inter-comparison among different satellite instruments [6].

3.A.   *Validation of the ROLO Model over Time*

From the launch of the SeaWiFS through mid-2007 the OBPG CVT developed and applied a set of empirically-derived geometric corrections to the low-phase SeaWiFS lunar calibration time series [7], comprised of 114 lunar observations collected over a 10 year time span between November 1997 and May 2007. The individual lunar observations were normalized to a common viewing geometry by applying corrections for the Sun-Moon and SeaWiFS-Moon distances, variations in phase angle, and variations in libration angles. The empirical phase correction was computed by fitting a quadratic function of the phase (over the phase angle range of $-6.0°$ to $-8.0°$ and $+5.0°$ to $+10.0°$) to the lunar reflectance normalized to a value of unity at a phase angle of $7°$. The empirical libration corrections were computed by performing multiple regressions of the subspacecraft longitude and latitude and the subsolar longitude and latitude against the lunar time series. The OBPG CVT also processed the lunar time series through the ROLO model. The empirical corrections, when applied to the low phase lunar observations, yielded a geometrically-corrected lunar time series that was statistically indistinguishable from the lunar time series with geometric corrections provided by the ROLO model [7,9]. The Sun-Moon and SeaWiFS-Moon distances, phase angles, and libration angles derived from the empirical corrections and from the ROLO model were the same. The OBPG used this comparison between the SeaWiFS empirical geometric corrections and the ROLO model output to validate the performance of the ROLO model over time, though over the limited phase angle range of the SeaWiFS low phase angle lunar observations. For the fifth global reprocessing of the SeaWiFS ocean color products, completed in July 2007, the OBPG CVT adopted the ROLO model as the primary method for performing geometric corrections for the SeaWiFS lunar data. One advantage of this change in methodology is that using the ROLO model for the geometric corrections extends the phase angle range over which the SeaWiFS lunar data could be calibrated.

4. Comparison of SeaWiFS, Terra MODIS, and Aqua MODIS over Wavelength

The cross calibration of SeaWiFS, Terra MODIS, and Aqua MODIS over wavelength, to determine the on-orbit calibration biases between the instruments, is made through a mission-long comparison of the primary lunar calibration data set for each instrument: the low phase angle observations for SeaWiFS ($-7°, +7°$), the scheduled observations for Terra MODIS ($+55°$) and the scheduled observations for Aqua MODIS ($-55°$). Each instrument has the latest on-orbit calibration applied to the lunar data, providing stable TOA irradiances of the Moon for the comparison. This cross calibration is performed using the mission-averaged ROLO residuals for each instrument and band, as shown in Table 3, in Table 4, and as plotted in Fig. 6. For all three instruments, the residuals of the lunar observations from the ROLO model do not show any systematic trends with wavelength. The observed biases between the instruments arise primarily from differences in the prelaunch calibration of each instrument. The sources of uncertainty in these comparisons are:

1) The observational scatter in the data for each instrument and band.

2) Any residual RVS error for SeaWiFS, since the SeaWiFS observations were made over a range of scan angles. The uncertainty in the SeaWiFS RVS correction is 0.3% [10]. The MODIS primary lunar observations were made at a constant AOI on the primary mirror, so RVS errors for MODIS do not contribute to the uncertainty in the comparisons.

3) Any residual phase dependence in the ROLO model, since the three sets of observations were made at different phase angles. The residual phase dependence is given as no greater than 1% over the phase angle range of the model [6].

The root-sum-square combination of these uncertainties are reported as the errors on the biases in Table 3 and Table 4. The largest uncertainties in the biases involves Terra MODIS Band 8 (412 nm), which has the largest on-orbit calibration uncertainty. The mean value of the uncertainties for the Terra and Aqua biases is $1.18 \pm 0.13\%$; the mean plus one standard deviation is 1.3%, which is a robust estimate of the overall uncertainty in the MODIS biases. The mean value of the uncertainties for the SeaWiFS and Terra biases is $1.26 \pm 0.11\%$; the mean plus one standard deviation is 1.4%, which is a robust estimate of the overall uncertainty in the SeaWiFS and Terra biases. The mean value of the uncertainties for the SeaWiFS and Aqua biases is $1.21 \pm 0.04\%$; the mean plus one standard deviation is 1.3%, which is a robust estimate of the overall uncertainty in the SeaWiFS and Aqua biases. The cross calibration results for Terra and Aqua MODIS are comparable to the lunar calibration-derived biases reported previously for two MODIS instruments by MCST [11]. These results are also comparable to surface reflectance-based vicarious calibration results for Terra and Aqua MODIS at Railroad Valley [12].

On 14 April 2003, Terra MODIS and SeaWiFS made near-simultaneous observations of the Moon as part of the EOS Lunar Cross Calibration Experiment [3]. A target lunar phase

angle of $-28°$ was chosen by the EOS Project to facilitate the simultaneous observations and to remove any phase dependence from the cross calibration. SeaWiFS performed a standard lunar calibration at the cross calibration time, while the Terra spacecraft performed a deep space maneuver so MODIS viewed the Moon through its nadir aperture. The actual times and phase angles of the lunar observations are shown in Table 2, while the instrument comparison is shown in the second plot of Fig. 6. The third plot of the figure, comparing the residuals at $-27°$ phase with the residuals at the primary phase angles, shows a reduced bias between the two instruments at $-27°$ compared to the bias for the primary observations. The sources of uncertainty for the Lunar Cross Calibration Experiment are different from those of the primary SeaWiFS and Terra MODIS lunar observations. Since the SeaWiFS and Terra MODIS lunar measurements were made at essentially the same phase angle for this experiment, any residual phase dependence in the ROLO model would not affect the comparison. The sources of uncertainty in these comparisons are:

1) The experiment yielded a single lunar observation for each instrument. The uncertainty due to observational scatter for this observation for each instrument and band is assumed to be the same as for the mission-long comparisons.

2) The uncertainty in the SeaWiFS RVS correction of 0.3% [10].

3) The difference in the AOI of the Terra MODIS observation. For this experiment Terra MODIS observed the Moon through the nadir aperture rather than through the space view port. This difference in the AOI of the lunar observations should be accounted for by the RVS correction of the data. The uncertainty in the Terra RVS correction is 0.5% [13, 14].

The root-sum-square combination of these uncertainties are reported as the errors on the biases in Table 5. The SeaWiFS / Terra MODIS bias uncertainties range from 0.9% to 1.2%, with the largest uncertainty again involving Terra MODIS Band 8. The mean value of the uncertainties for the SeaWiFS and Terra biases is $0.96 \pm 0.11\%$; the mean plus one standard deviation is 1.1%, which is a robust estimate of the overall uncertainty in the SeaWiFS and Terra biases. The decrease in the calibration biases between SeaWiFS and Terra MODIS at $-27°$ and the calibration biases for the observations at $7°$ and $55°$ are greater than the uncertainties in the respective sets of observations. This decrease in the biases between SeaWiFS and Terra MODIS for the $-27°$ observations raises the question of whether these observations show any residual phase dependence in the ROLO model. To investigate the phase independence of the model, the OBPG CVT and MCST have examined the full set of lunar observations for all three instruments over the phase angle range of the data, $-80°$ to $-6°$ and $+5°$ $+82°$ (Table 2).

4.A. Validation by Vicarious Calibration Comparison

The vicarious calibration of ocean color products from Earth remote sensing instruments adjusts the on-orbit calibration of the instruments to match the system-level calibration of the

in situ radiometer and atmospheric correction algorithm [15]. Accordingly, comparison of the derived vicarious gains provides a cross-calibration opportunity for the satellite instruments. The OBPG CVT optimizes the ocean color products for SeaWiFS and MODIS through the vicarious calibration of the ocean color bands:

1) The calibration of the 865 nm band (SeaWiFS band 8; MODIS band 16) is assumed to be correct.

2) The 765 nm band (SeaWiFS band; MODIS band 15) is calibrated relative to the 865 nm band to retrieve the expected aerosols over open ocean scenes.

3) The top-of-the-atmosphere radiances computed for the visible bands are calibrated against in water measurements from the Marine Optical Buoy (MOBY), propagated to the top of the atmosphere using the retrieved atmospheric correction parameters.

The vicarious calibration process provides a means of comparing the on-orbit calibration of SeaWiFS and both MODIS instruments using the MOBY spectroradiometer in conjunction with the atmospheric correction algorithm as a transfer radiometer [9].

The vicarious gains derived for the ocean color bands of all three instruments for the 2009 reprocessing of the global ocean color data sets are shown in Table 6 and are plotted in Fig. 7. The inverses of the vicarious gains are plotted so that the SeaWiFS or MODIS measurement is in the numerator of the ratios, allowing comparisons with the lunar observations. Comparison of the vicarious gains in Fig. 7 with the lunar residuals in Fig. 6 shows that the variations in the vicarious gains as a function of wavelength are comparable to the variations in the lunar residuals for all three instruments. The reduction of the biases in the vicarious gains, compared to the lunar calibration biases, results primarily from the way the vicarious calibration process handles the 865 nm atmospheric correction bands. The vicarious calibration process implicitly assumes that all three instruments retrieve the same aerosol radiances with these bands when observing the same open ocean scenes. This process reduces the calibration biases for the 865 nm bands, which has the effect of reducing the biases for all of the ocean color bands. As is shown in Table 6, the uncertainties in the vicarious calibration biases between SeaWiFS and either MODIS instrument are 1.2% and the uncertainties in the vicarious calibration biases between Terra MODIS and Aqua MODIS are 1.3%. These uncertainties on the biases are comparable to those derived for the lunar calibration biases (1.3% for the Terra MODIS / Aqua MODIS biases, 1.4% for the Terra MODIS / SeaWiFS biases, and 1.3% for the Aqua MODIS / SeaWiFS biases). Accordingly, the vicarious calibration of SeaWiFS, Terra MODIS, and Aqua MODIS is consistent with the cross calibration of these three instruments using the lunar observations, with the vicarious gains mitigating the calibration biases of the ocean color bands.

4.B.   Summary of the Cross Calibration over Wavelength

The lunar cross calibration results show that Terra MODIS and Aqua MODIS agree, band-to-band, at the 1-3% level, while SeaWiFS and either MODIS instrument agree at the 3-8%

level. The combined uncertainties for these comparisons are 1.3% for Terra and Aqua MODIS, 1.4% for SeaWiFS and Terra MODIS, and 1.3% for SeaWiFS and Aqua MODIS. These cross calibration results are consistent with the vicarious calibration of ocean color products for these instruments, with the vicarious gains mitigating the calibration biases for the ocean color bands.

5. Comparison of SeaWiFS, Terra MODIS, and Aqua MODIS over Phase Angle

The OBPG CVT and MCST have undertaken a comparison of the full set of SeaWiFS and MODIS lunar observations over their respective missions as a function of phase angle. The primary goal of this analysis is to determine if the SeaWiFS low-phase ($\pm 7°$) observations can be compared directly with the MODIS scheduled observations ($\pm 55°$ phase). While the comparisons were made for all of the bands shown in Table 1, we present the results of the comparison for the 412 nm bands (SeaWiFS Band 1 and MODIS Band 8). The behavior of these bands is representative of the phase angle response of the other bands.

For this comparison, Fig. 8 shows the full set of lunar observations (from Table 2) for each instrument. The SeaWiFS high phase observations are clustered at the phase angles selected to investigate residual phase effects in the ROLO model and selected to replicate the $-27°$ phase observation of the Lunar Cross Calibration Experiment. Examination of these plots shows the inherent scatter in a single lunar measurement. For SeaWiFS, the scatter in the observations most likely arises from the uncertainties in the oversampling correction. For both MODIS instruments the unscheduled observations are obtained at higher phase angles than the scheduled observations, with a corresponding increase in the scatter in the data. A likely cause of this increased scatter is that at phase angles greater than $55°$, the lunar phase function becomes so small that the low illumination levels start to increase the uncertainty of the observations. It should be noted that the amount of scatter in the lunar observations for each of the bands for all three instruments is comparable.

To facilitate the comparison of these data sets as a function of phase angle and to minimize the impact of the scatter in a single observation, we have binned the residuals at a set of selected phase angles over the full range of the data For SeaWiFS, the mean residuals are computed for the low phase observations on either side of full phase and for clusters of high phase observations. For the two MODIS instruments, the mean residuals are computed for $10°$ bins. The phase angle of each bin is the mean of the phase angle of the observations that went into that bin. Fig. 8 and Table 7 show the mean residuals and standard deviations plotted versus phase angle for each wavelength. The Lunar Cross Calibration Experiment residuals for SeaWiFS and Terra MODIS are plotted at $-27°$ phase without any error bars. For SeaWiFS, the mean residuals show a trend with phase before full phase, but the standard deviations increase as well. For both MODIS instruments, the residuals for the unscheduled lunar observations are slightly larger than those for the scheduled measurements, with larger standard deviations as well.

In comparing the two plots in Fig. 8, we see that for SeaWiFS, the Lunar Cross Calibration Experiment data points fall near the upper end of the range for the $-28°$ bin; this agree-

ment is expected since these binned observations attempted to replicate the cross calibration measurement. For Terra MODIS the cross calibration data points fall within the range of the remaining lunar observations. For all three instruments, these results are similar for the other wavelengths.

The goal of this analysis over phase angle is to set an observational upper limit on any residual phase dependence in the ROLO model based on the lunar data comparisons. This upper limit arises from the uncertainties in the input data sets: the scatter in the observations for a particular phase angle bin, the bias for the bin, and the uncertainties in the SeaWiFS RVS correction. The bias for a given bin is the difference between the mean value for that bin and mean value from the comparison with wavelength (Table 3 and Table 4). The uncertainties for each instrument are presented in Table 7. The uncertainty in the SeaWiFS RVS correction is 0.3% [10].

The SeaWiFS, Terra MODIS, and Aqua MODIS sample three separate ranges of the phase angle space of the ROLO model, so the observational constraint on any residual phase angle dependence in the model will be examined on a per-instrument basis. For Aqua MODIS the limit on the phase dependence of the model over the phase angle range of $-80°$ to $-51°$ is the 1.1% uncertainty from the $-74°$ bin. For Terra MODIS, the limit on the phase dependence of the model over the phase angle range of $+52°$ to $+82°$ is the 1.5% uncertainty from the $+74°$ bin. In addition, the challenges of calibrating Terra MODIS have resulted in the larger uncertainties occurring after full phase. For SeaWiFS, the uncertainties are larger for the high phase angle observations, with the measurements before full phase having the largest uncertainty. Since the SeaWiFS and Terra MODIS uncertainties at $+56°$ are comparable (0.9% and 1.0%), the SeaWiFS 1.7% uncertainty at $-45°$ probably arises from the oversampling correction of these high phase observations. The mean value of the uncertainties for the eight SeaWiFS phase angle bins is $1.00 \pm 0.43\%$; the mean plus one standard deviation is 1.5%. Condequently, the uncertainty of 1.7% at $-45°$ is a robust estimate of the limit on the phase dependence of the model over the phase angle range of $-45°$ to $-6°$ and $+5°$ to $+56°$. The constraints from the MODIS instruments are smaller than this value. Consequently, over the phase angle range of the data, $-80°$ to $-6°$ and $+5°$ to $+82°$, the SeaWiFS, Terra MODIS, and Aqua MODIS lunar cross calibration shows that any residual phase dependence in the ROLO model output is 1.7% or less. The difference between this observational contraint on the residual phase dependence of the ROLO model and the uncertainty in the model (1% [6]) is not unexpected, since the ROLO model was derived from a larger ground-based data set [4]. The lunar phase functions at 412 nm, 555 nm, and 865 nm vary by factors of 8.8, 8.0, and 7.1 over the phase angle range of 5° to 82°, as shown in Fig. 5, so a 1.7% limit on the phase dependence represents a significant validation of the phase independence of the ROLO model using on-orbit data.

6. Discussion and Implications of Cross Calibration Results

Observations of the Moon, facilitated by the ROLO model, provide robust estimates of the relative biases in the on-orbit calibration of remote sensing instruments at the top of the

atmosphere, where complications of atmospheric correction algorithms can be avoided. A limitation in using this approach to cross calibration are instrument bands that saturate on the Moon. The cross calibration results show that Terra MODIS and Aqua MODIS agree, band-to-band, at the 1-3% level, while SeaWiFS and either MODIS instrument agree at the 3-8% level. The combined uncertainties in the cross calibration comparisons are 1.3% between Terra MODIS and Aqua MODIS, 1.4% between SeaWiFS and Terra MODIS, and 1.3% between SeaWiFS and Aqua MODIS. The lunar cross calibration results are consistent with the gains derived from the vicarious calibration of ocean color products for these instruments, with the vicarious gains mitigating the calibration biases for the ocean color bands. The comparison of the lunar cross calibration results with the vicarious calibration results, and the uncertainty analysis presented here, lead us to conclude that the most likely source of the calibration biases between these three instruments are differences in the prelaunch calibrations of the instruments, which have 5% uncertainties on the absolute radiance calibration [10, 11]

Since the SeaWiFS, Terra MODIS, and Aqua MODIS lunar calibrations cover a broad phase angle range, a primary uncertainty in the cross calibration comaprison would be any residual phase dependence in the USGS ROLO photometric model of the Moon. The residual phase dependence in the ROLO model is given as less than 1% [6], while the observational constraint from this cross calibration comparison is that the residual phase dependence is less than 1.7% over a phase angle range of $-80°$ to $-6°$ and $+5°$ to $+82°$. The OBPG CVT set the the phase angle of the primary SeaWiFS lunar observations at $7°$ to maximize the illuminated surface of the Moon while avoiding the opposition effect at small phase angles [16]. At large phase angles, the low amount of light reflected by the Moon becomes a consideration in the uncertainty of the lunar observations. Consequently, MCST determined that a phase angle of $55°$ balanced the mission requirement of minimizing the rolls of the spacecraft to observe the Moon to less than $20°$ with the requirement of observing the Moon with sufficient illumination to minimize the uncertainy in the observations [17]. For SeaWiFS and MODIS, the robustness of the ROLO model allows lunar observations to provide highly precise information about the relative change in radiometric performance of the instruments over time. By minimizing the phase angle range of the primary lunar observations, the OBPG CVT has achieved a long-term stability for SeaWiFS TOA radiances of 0.1% over its mission lifetime [1, 7].

The results of this cross calibration study have implications for upcoming remote sensing instruments, such as VIIRS on the NPOESS Preparatory Project (NPP) satellite. The primary application to VIIRS concerns the requirement for lunar calibration roll maneuvers for the NPP spacecraft. MODIS views the Moon during most of the year without roll maneuvers, though over a range of phase angles; the same circumstances exist for VIIRS. This study shows that the ROLO lunar model can be used to calibrate lunar observations over the expected phase angle range to within a 1.7% uncertainty. Since a radiometric stability better than 0.5% is required to produce climate-quality ocean color data, minimizing the phase angle range of the lunar observation minimizes the uncertainty in the calibration due

to residual phase errors in the ROLO model output. One of the issues for VIIRS is that the space view is narrower for VIIRS ($\sim 0.85°$) than for MODIS ($\sim 4.1°$). This means that, without roll maneuvers, only part of the Moon will be viewed by VIIRS for most months [18]. Small rolls of the spacecraft of a few degrees are required for VIIRS to view the complete lunar disk at every available opportunity, and larger rolls of up to 15° are required to view the Moon at a constant phase angle of 55°. Having VIIRS observe the Moon at a phase angle of 55° would facilitate the cross calibration of VIIRS with MODIS.

The results of this study also have implications for instruments currently being designed for the NASA Decadal Survey missions:

1) The cross calibration of SeaWiFS, Terra MODIS, and Aqua MODIS demonstrates the importance of the USGS ROLO photometric model of the Moon to the on-orbit calibration of remote sensing satellite instruments. The ROLO model allows a determination of the on-orbit performance of an instrument to be made with a minimal number of lunar observations. Consequently, the model should be maintained and updated to support future instruments.

2 Future instruments that use lunar observations as part of their on-orbit calibration strategy should be designed with reflective solar bands that do not saturate on the Moon. Saturation on the Moon has hampered the on-orbit calibration of MODIS bands $13 - 16$. One way to avoid saturation for high-sensitivity bands is to use multiple gains for these bands, as have been used by SeaWiFS and VIIRS; this approach requires monitoring of possible gain drifts, as have been observed for SeaWiFS [19,20]. Another approach would be to design the dynamic range of these bands to cover the required radiance range; such an approach would likely require the use of 14-bit analog-to-digital converters in order to maintain the required radiometric sensitivity over the oceans, with the corresponding increase in data volume. The tradeoffs for any aproach would have to be evaluated.

3) Future spacecraft should be designed with attitude control systems that maintain knowledge of pitch and roll rates throughout lunar calibration maneuvers. Such knowledge would facilitate the computation of any needed oversampling corrections.

4) The operations concepts for upcoming instruments should be designed to maximize the number of lunar observations over the mission time frame, while minimizing the phase angle range of the observations. Lunar observations obtained on a monthly basis allow the instrument performance to be closely monitored. Minimizing the phase angle range of the observations removes one source of uncertainty in the on-orbit calibration data set.

The implementation of these design considerations would allow the optimum calibration of future instruments to be derived on orbit, which would provide the long-term radiometric stability for top-of-the-atmosphere radiances required for climate research.

Acknowledgments

References

1. J. Sun, R.E. Eplee, Jr., X. Xiong, T. Stone, G. Meister, and C.R. McClain, "MODIS and SeaWiFS on-orbit lunar calibration," in *Earth Observing Systems XIII*, J.J. Butler and J. Xiong, eds., *Proc. SPIE* **7081**, 70810Y, 2008.

2. R.E. Eplee, Jr., X. Xiong, J.-Q. Sun, G. Meister, and C.R. McClain, "The cross calibration of SeaWiFS and MODIS using on-orbit observations of the Moon," in *Earth Observing Systems XIV*, J.J. Butler, X. Xiong, and X. Gu, eds., *Proc. SPIE* **7452**, 74520X, 2009.

3. J.J. Butler, "On-orbit cross-calibration of AM satellite remote sensing instruments using the Moon," presented at the International Workshop on Radiometric and Geometric Calibration, Gulfport, Mississippi, December 2-5, 2003.

4. H.H. Kieffer and T.C. Stone, "The spectral irradiance of the Moon," *Astron. J.* **129**, 2887–2901, 2005.

5. T.C. Stone and H.H. Kieffer, "Use of the Moon to support on-orbit sensor calibration for climate change measurements," in *Earth Observing Systems XI*, J.J. Butler and J. Xiong, eds., *Proc. SPIE* **6296**, 62960Y, 2006.

6. T.C. Stone, "Radiometric calibration stability and inter-calibration of solar-band instruments in orbit using the Moon," in *Earth Observing Systems XIII*, J.J. Butler and J. Xiong, eds., *Proc. SPIE* **7081**, 70810X, 2008.

7. R.E. Eplee, Jr., R.A. Barnes, F.S. Patt, G. Meister, and C.R. McClain, "SeaWiFS lunar calibration methodology after six years on orbit," in *Earth Observing Systems IX*, W.L. Barnes and J.J. Butler, eds., *Proc. SPIE* **5542**, 1–13, 2004.

8. J. Sun, X. Xiong, W.L. Barnes, and B. Guenther, "MODIS reflective solar bands on-orbit lunar calibration," *IEEE Trans. Geosci. Remote Sens.* **45**, 2383–2393, 2007.

9. R.E. Eplee, Jr., S.W. Bailey, R.A. Barnes, H.H. Kieffer, and C.R. McClain, "Comparison of SeaWiFS on-orbit lunar and vicarious calibrations," in *Earth Observing Systems XI*, J.J. Butler and J. Xiong, eds., *Proc. SPIE* **6296**, 629610, 2006.

10. R.A. Barnes, A.W. Holmes, W.L. Barnes, W.E. Esaias, C.R. McClain and T. Svitek, *SeaWiFS Prelaunch Radiometric Calibration and Spectral Characterization*, NASA Tech.

Memo. 104566 **23**, S.B. Hooker, E.R. Firestone, and J.G. Acker, eds., (NASA Goddard Space Flight Center, Greenbelt, Maryland), 55 pp., 1994.

11. X. Xiong, J. Sun, and W. Barnes, "Intercomparison of on-orbit calibration consistency between Terra and Aqua MODIS reflective solar bands using the Moon," *IEEE Geosci. Remote. Sens. Lett.* **5**, 778-782, 2008.

12. K. Thome, J. Czapla-Meyrs, and S. Biggar, "Vicarious calibration of Aqua and Terra MODIS," in *Earth Observing Systems VIII*, W.L. Barnes, ed., *Proc. SPIE* **5151**, 395-405, 2003.

13. C. Pan, J. Xiong, and N. Che, "MODIS Pre-launch reflective solar band response vs. scan angle," in *Earth Observing Systems XII*, J.J. Butler and J. Xiong, eds., *Proc. SPIE* **6677**, 66770R, 2007.

14. J. Sun, X. Xiong, H. Chen, A. Angai, X. Geng, and A. Wu, "Time-dependent response versus scan angle for the MODIS reflective solar bands", in *Earth Observing Systems XIV*, J.J. Butler, X. Xiong, and X. Gu, eds., *Proc. SPIE* **7452**, 745219, 2009.

15. B.A. Franz, S.W. Bailey, P.J. Werdell, and C.R. McClain, "Sensor-independent approach to the vicarious calibration of satellite ocean color radiometry," *Appl. Opt.* **46**, 5068–5082, 2007.

16. R.A. Barnes, R.E. Eplee, Jr., F.S. Patt, and C.R. McClain, "Changes in the radiometric sensitivity of SeaWiFS determined from lunar and solar-based measurements," *Appl. Opt.* **38**, 4649-4664, 1999.

17. J. Sun, X. Xiong, B. Guenther, and W. Barnes, "Radiometric stability monitoring of the MODIS reflective solar bands using the Moon," *Metrologia* **40**, S85-S88, 2003.

18. F.S. Patt, R.E. Eplee, R.A. Barnes, G. Meister, and J.J. Butler, "Use of the Moon as a calibration reference for NPP VIIRS," in *Earth Observing Systems X*, J.J. Butler, ed., *Proc. SPIE* **5882**, 588215, 2005.

19. R.E. Eplee, Jr., F.S. Patt, G. Meister, B.A. Franz, S.W. Bailey, and C.R. McClain, "The on-orbit calibration of SeaWiFS: Revised temperature and gain corrections," in *Earth Observing Systems XII*, J.J. Butler and J. Xiong, eds., *Proc. SPIE* **6677**, 66770E, 2007.

20. R.E. Eplee, Jr., F.S. Patt, B.A. Franz, S.W. Bailey, G. Meister, and C.R. McClain, "SeaWiFS on-orbit gain and detector calibrations: effects on ocean products," *Appl. Opt.* **46**, 6733-6750, 2007.

Table 1. **SeaWiFS and MODIS Band Comparisons.** *MODIS ocean color bands which saturate on the Moon.

SeaWiFS	λ (nm)	Bandwidth	MODIS	λ (nm)	Bandwidth
Band 1	412	402–422	**Band 8**	412	405–420
Band 2	443	433–453	**Band 9**	443	438–448
			Band 3	469	459–479
Band 3	490	480–500	**Band 10**	488	483–493
Band 4	510	500-520	**Band 11**	531	526–536
Band 5	555	545–565	**Band 12**	551	546–556
			Band 4	555	545–565
Band 6	670	660–680	**Band 1**	645	620–670
			Band 13*	667	662–672
			Band 14*	678	673–683
Band 7	765	745-785	**Band 15***	748	743–753
Band 8	865	845–885	**Band 2**	858	841–876
			Band 16*	869	862–877

Table 2. **Lunar Observations.** *Data set used as the primary radiometric stability monitor. [a]SeaWiFS cals between $+6°$ and $+8°$. [b]Terra cals between $+54°$ and $+56°$. [c]Aqua cals between $-54°$ and $-56°$.

Instrument	Type	Phase Angle	Number	Time Range
SeaWiFS	Low Phase*	-6.0 to -8.0	83	Nov 97 – Apr 09
	-7.0, +7.0 nominal	+5.0 to +10.0	49 (38[a])	
	Cross Cal	-27.1	1	14 Apr 03 22:34:21 UT
	High Phase	-27.0 to -49.0	26	Jul 04 – Dec 07
		+27.0 to +66.0	32	
Terra MODIS	Scheduled*	+52.0 to +62.0	82 (73[b])	Mar 00 – Feb 09
	+55.0 nominal			
	Cross Cal	-27.7	1	14 Apr 03 22:09:35 UT
	Unscheduled	+55.0 to +82.0	297	Jul 00 – Dec 08
Aqua MODIS	Scheduled*	-51.0 to -58.0	61 (50[c])	Jun 02 – Apr 09
	-55.0 nominal			
	Unscheduled	-54.0 to -80.0	171	Dec 02 – Dec 08

Table 3. **Terra MODIS / Aqua MODIS Biases.** The errors on the MODIS/ROLO ratios are standard deviations of the means of the observations. The errors on the biases are the combined scatter for the two instruments and the ROLO phase uncertainty.

Band	Band Center (nm)	Terra/ROLO	Aqua/ROLO	Bias (%)
8	412	1.082 ± 0.009	1.075 ± 0.006	0.7 ± 1.5
9	443	1.080 ± 0.006	1.065 ± 0.004	1.3 ± 1.2
3	469	1.010 ± 0.004	1.069 ± 0.005	2.8 ± 1.2
10	488	1.099 ± 0.004	1.082 ± 0.004	1.6 ± 1.1
11	531	1.091 ± 0.004	1.063 ± 0.003	2.7 ± 1.1
12	551	1.103 ± 0.004	1.083 ± 0.003	1.8 ± 1.1
4	555	1.088 ± 0.004	1.058 ± 0.003	2.8 ± 1.1
1	645	1.056 ± 0.004	1.063 ± 0.003	0.7 ± 1.1
2	858	1.075 ± 0.006	1.082 ± 0.003	0.7 ± 1.2

Table 4. **SeaWiFS / MODIS Biases.** The errors are on the SeaWiFS/ROLO ratios are standard deviations of the mean of the observations. The errors on the biases are the combined scatter for the two instruments, the ROLO phase uncertainty, and the SeaWiFS RVS uncertainty.

SeaWiFS	MODIS	Band Centers (nm)	SeaWiFS/ROLO	Terra Bias (%)	Aqua Bias (%)
Band 1	Band 8	412 , 412	1.025 ± 0.006	5.6 ± 1.5	4.9 ± 1.3
Band 2	Band 9	443 , 443	1.024 ± 0.005	5.4 ± 1.3	4.0 ± 1.2
Band 3	Band 10	490 , 488	1.037 ± 0.005	6.0 ± 1.2	4.3 ± 1.2
Band 4	Band 11	510 , 531	1.029 ± 0.005	6.0 ± 1.2	3.3 ± 1.2
Band 5	Band 12	555 , 551	1.022 ± 0.005	7.8 ± 1.2	5.9 ± 1.2
Band 5	Band 4	555 , 555	1.022 ± 0.005	6.4 ± 1.2	3.5 ± 1.2
Band 6	Band 1	670 , 645	1.025 ± 0.005	3.0 ± 1.2	3.8 ± 1.2
Band 7		765	1.046 ± 0.005		
Band 8	Band 2	865 , 858	1.006 ± 0.006	6.8 ± 1.3	7.5 ± 1.2

Table 5. **SeaWiFS / Terra MODIS Cross Calibration Biases.** The observational scatter assumed for these single observations is the scatter from the mission-averages for the corresponding instrument/band. The errors on the biases are the combined scatter for the two instruments, the SeaWiFS RVS uncertainty, and the Terra RVS uncertainty.

SeaWiFS	MODIS	Band Centers (nm)	SeaWiFS/ROLO	Terra/ROLO	Bias (%)
Band 1	Band 8	412 , 412	1.042 ± 0.006	1.056 ± 0.009	1.5 ± 1.2
Band 2	Band 9	443 , 443	1.040 ± 0.005	1.061 ± 0.006	2.0 ± 1.0
	Band 3	469		1.069 ± 0.004	
Band 3	Band 10	490 , 488	1.052 ± 0.005	1.094 ± 0.004	4.0 ± 0.9
Band 4	Band 11	510 , 531	1.045 ± 0.005	1.067 ± 0.004	2.1 ± 0.9
Band 5	Band 12	555 , 551	1.038 ± 0.005	1.076 ± 0.004	3.6 ± 0.9
Band 5	Band 4	555 , 555	1.038 ± 0.005	1.054 ± 0.004	1.5 ± 0.9
Band 6	Band 1	670 , 645	1.042 ± 0.005	1.038 ± 0.004	0.4 ± 0.9
Band 7		765	1.059 ± 0.005		
Band 8	Band 2	865 , 858	1.018 ± 0.006	1.069 ± 0.006	5.0 ± 1.0

Table 6. **SeaWiFS / MODIS Vicarious Gains.** The uncertainties on the vicarious gains are 0.008 for SeaWiFS and 0.009 for either MODIS instrument. The uncertainties on the biases are the combined errors for the two instruments, SeaWiFS and either MODIS.

SeaWiFS	MODIS	SeaWiFS Gain	Terra Gain	Aqua Gain	S/T Bias (%)	S/A Bias (%)	T/A Bias (%)
Band 1	Band 8	1.0041	0.9990	0.9768	0.5 ± 1.2	2.8 ± 1.2	2.3 ± 1.3
Band 2	Band 9	0.9952	0.9961	0.9936	0.09 ± 1.2	0.2 ± 1.2	0.3 ± 1.3
	Band 3		1.0012	1.0113			1.0 ± 1.3
Band 3	Band 10	0.9873	0.9987	0.9972	1.1 ± 1.2	1.0 ± 1.2	0.2 ± 1.3
Band 4	Band 11	0.9903	0.9947	0.9946	0.4 ± 1.2	0.4 ± 1.2	0.01 ± 1.3
Band 5	Band 12	1.0022	0.9941	0.9950	0.8 ± 1.2	0.7 ± 1.2	0.09 ± 1.3
Band 5	Band 4	1.0022	0.9945	0.9999	0.8 ± 1.2	0.2 ± 1.2	0.5 ± 1.3
Band 6	Band 1	0.9777	1.0282	1.0252	4.9 ± 1.2	4.6 ± 1.2	0.3 ± 1.3
Band 6	Band 13	0.9777	0.9926	0.9961	1.5 ± 1.2	1.8 ± 1.2	0.4 ± 1.3
Band 6	Band 14	0.9777	0.9979	0.9974	2.0 ± 1.2	1.9 ± 1.2	0.05 ± 1.3
Band 7	Band 15	0.9700	0.9974	0.9977	2.7 ± 1.2	2.8 ± 1.2	0.03 ± 1.3
Band 8	Band 2	1.0000	1.0161	1.0244	1.6 ± 1.2	2.4 ± 1.2	0.8 ± 1.3
Band 8	Band 16	1.0000	1.0000	1.0000			

Table 7. **Phase Angle Comparisons for 412 nm Bands.** The cross calibration results are presented for SeaWiFS band 1 and for MODIS band 8. The errors on the Inst/ROLO ratios are standard deviations of the mean of the observations. The number of observations is for the phase angle bin. The biases are the differences between the means and the mission-long average from Table 3 and Table 4. The combined errors are the scatter, the bias, and the RVS uncertainty for SeaWiFS.

| Phase	Inst	Number of Obs	Inst/ROLO (%)	Bias (%)	Combined Error (%)
−74°	A	60	1.080 ± 0.010	0.5	1.1
−65°	A	85	1.076 ± 0.008	0.1	0.8
−56°	A	87	1.076 ± 0.006	0.08	0.6
−45°	S	7	1.038 ± 0.011	1.3	1.7
−40°	S	11	1.035 ± 0.012	1.0	1.6
−28°	S	9	1.032 ± 0.007	0.8	1.1
−7°	S	83	1.025 ± 0.006	0.06	0.7
+7°	S	49	1.023 ± 0.005	0.1	0.6
+28°	S	6	1.024 ± 0.006	0.08	0.7
+45°	S	11	1.025 ± 0.006	0.04	0.7
+56°	S	15	1.025 ± 0.008	0.02	0.9
+56°	T	118	1.083 ± 0.010	0.1	1.0
+65°	T	123	1.085 ± 0.013	0.3	1.3
+74°	T	138	1.090 ± 0.013	0.8	1.5

List of Figure Captions

Fig. 1. SeaWiFS Band 1 Lunar Image. The difference between the spacecraft pitch rate across the Moon and the normal pitch rate across the Earth causes the elongated lunar image and necessitates the oversampling correction of the lunar data.

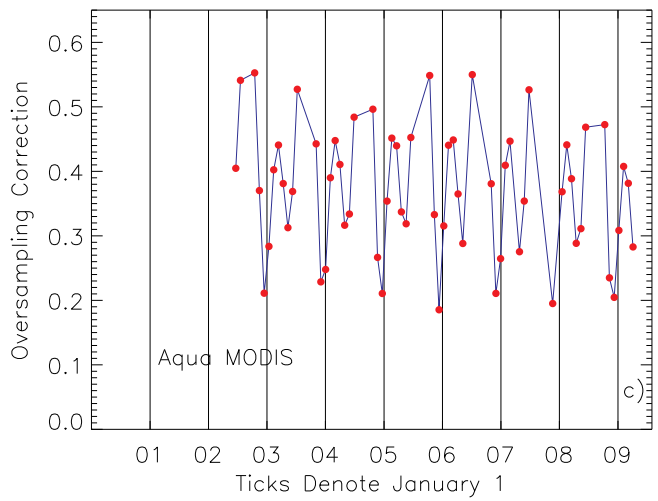**Fig. 2. Oversampling Correction Time Series.** a) SeaWiFS, b) Terra MODIS, and c) Aqua MODIS.

Fig. 3. Aqua MODIS Band 8 Lunar Image. The image on the right is the composite for detector 5 extracted from the image sequence on the left.

Fig. 4. MODIS Lunar Images. Band 2 (250 m resolution), Band 3 (500 m resolution), and Band 8 (1000 m resolution).

Fig. 5. Lunar Phase Functions. The phase functions of the Moon at wavelengths of 412, 555 and 865 nm, as derived by the ROLO model.

Fig. 6. SeaWiFS / MODIS Lunar Calibration Comparison. a) The three instrument mission-long band averages. b) The SeaWiFS / Terra MODIS EOS Lunar Calibration Experiment. c) The SeaWiFS / Terra MODIS mission-long averages and Lunar Calibration Experiment.

Fig. 7. SeaWiFS / MODIS Vicarious Calibration Comparison. The inverses of the vicarious gains are plotted so that the SeaWiFS or MODIS measurement is in the numerator of the ratios, allowing comparisons with the lunar observations.

Fig. 8. SeaWiFS / MODIS Mean Comparison as a Function of Phase Angle. a) The full lunar data sets are plotted for the 412 nm bands. b) The full data sets are binned and plotted as means with standard deviations for the 412 nm bands.
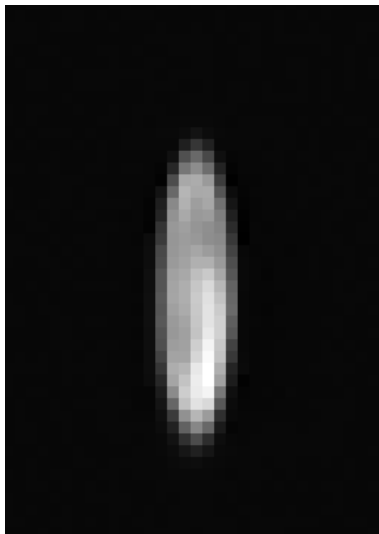
Fig. 1. **SeaWiFS Band 1 Lunar Image.** The difference between the space-craft pitch rate across the Moon and the normal pitch rate across the Earth causes the elongated lunar image and necessitates the oversampling correction of the lunar data. Eplee_LP130056_fig01.eps
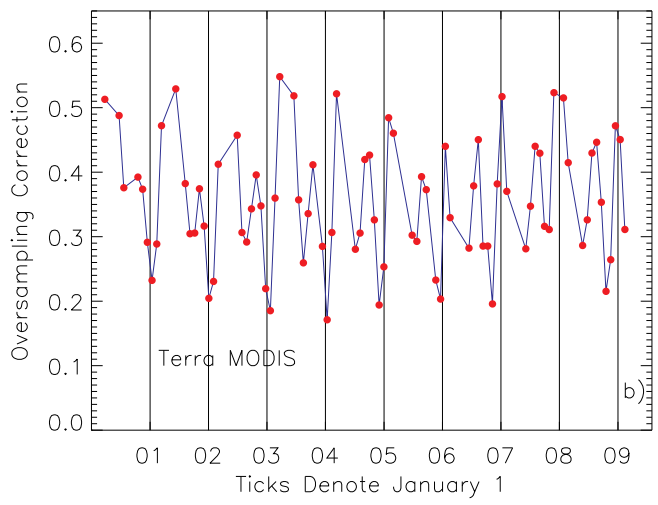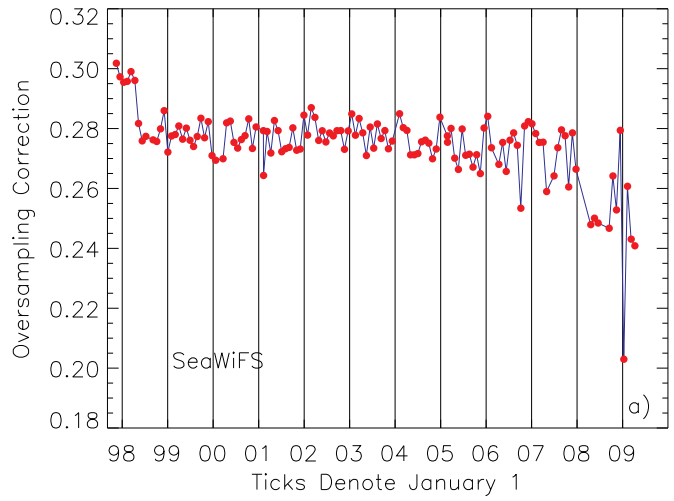
Fig. 2. **Oversampling Correction Time Series.** a) SeaWiFS, b) Terra MODIS, and c) Aqua MODIS. Eplee_LP130056_fig02a.eps, Eplee_LP130056_fig02b.eps, Eplee_LP130056_fig02c.eps
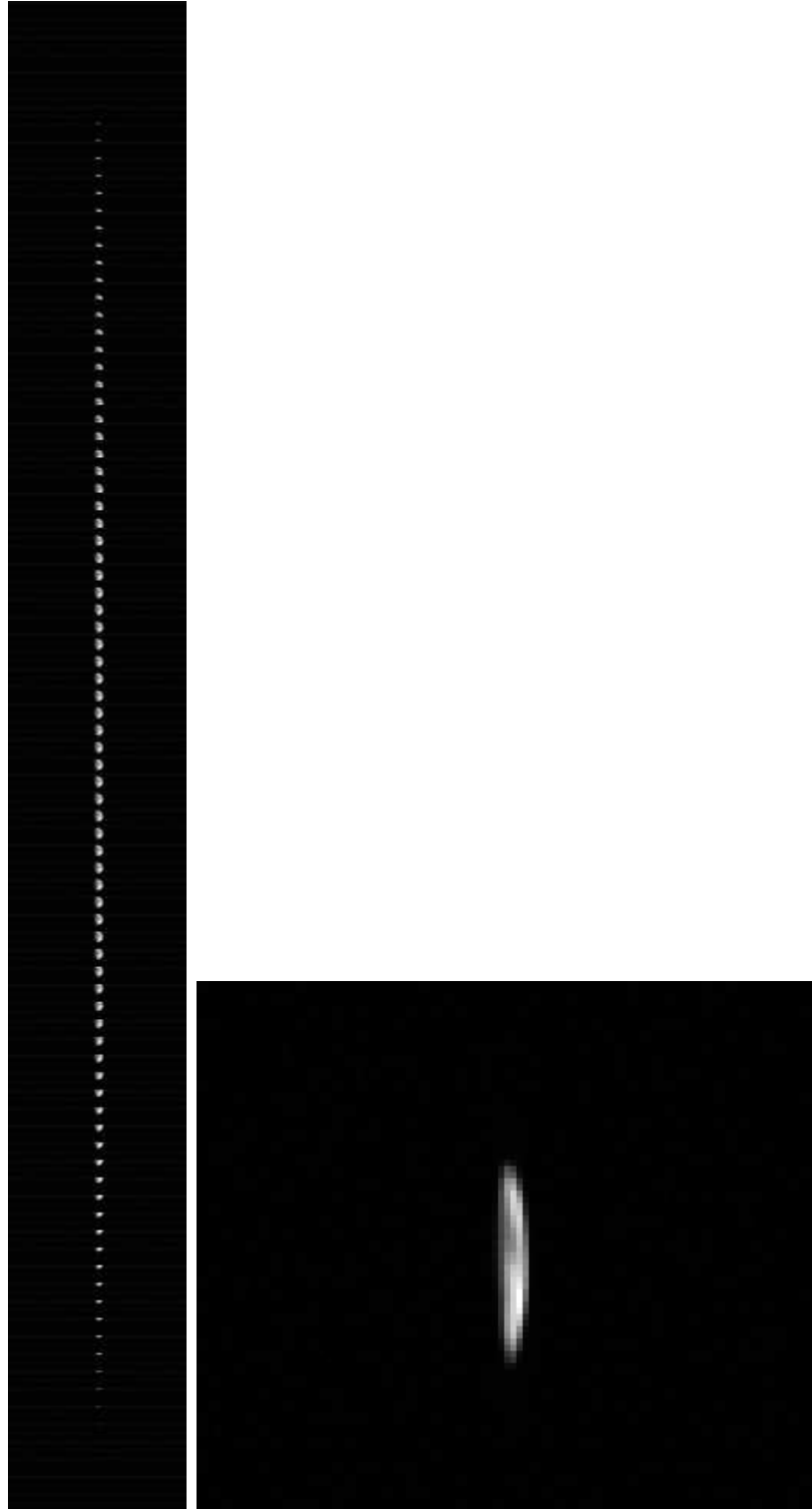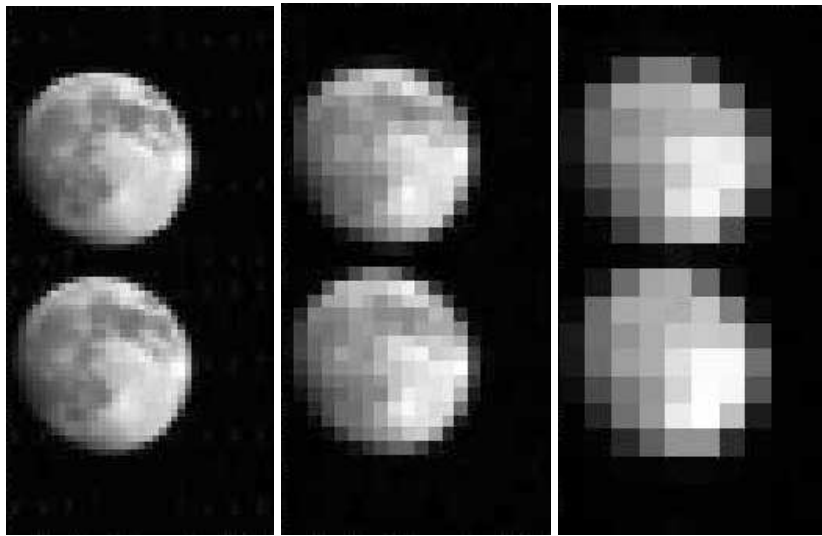
28

Fig. 3. **Aqua MODIS Band 8 Lunar Image.** The image on the right is the composite for detector 5 extracted from the image sequence on the left. Eplee_LP130056_fig03a.eps, Eplee_LP130056_fig03b.eps

Fig. 4. **MODIS Lunar Images.** Band 2 (250 m resolution), Band 3 (500 m resolution), and Band 8 (1000 m resolution). Eplee_LP130056_fig04a.eps, Eplee_LP130056_fig04b.eps, Eplee_LP130056_fig04c.eps
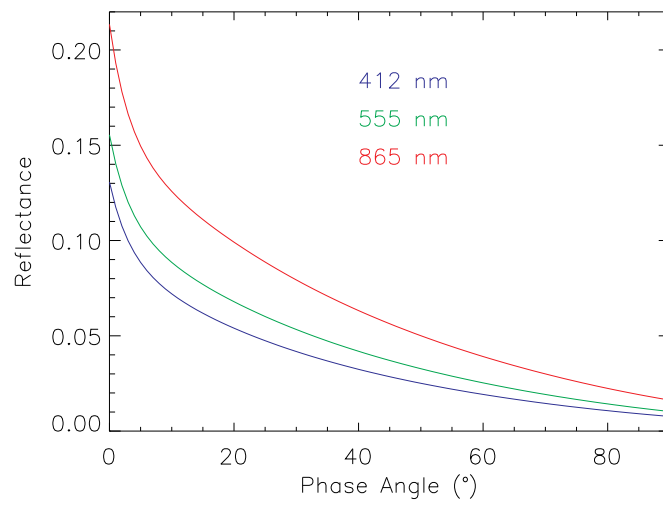
Fig. 5. **Lunar Phase Functions.** The phase functions of the Moon at wavelengths of 412, 555 and 865 nm, as derived by the ROLO model. Eplee_LP130056_fig05.eps
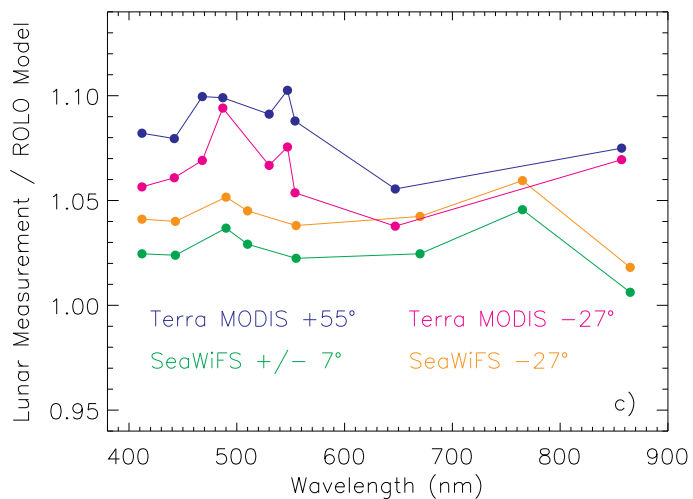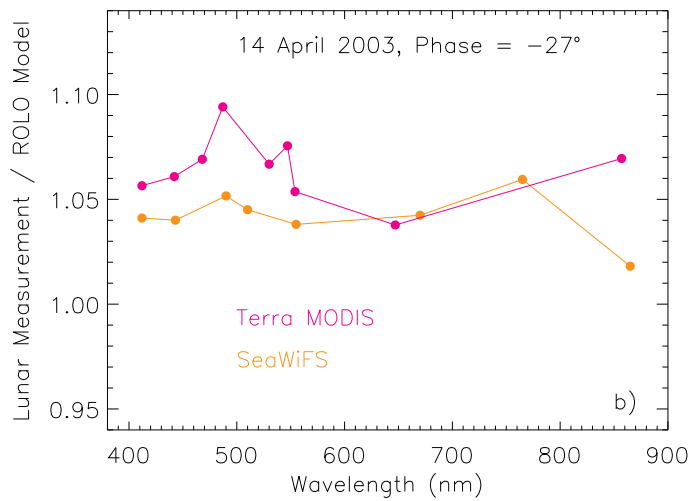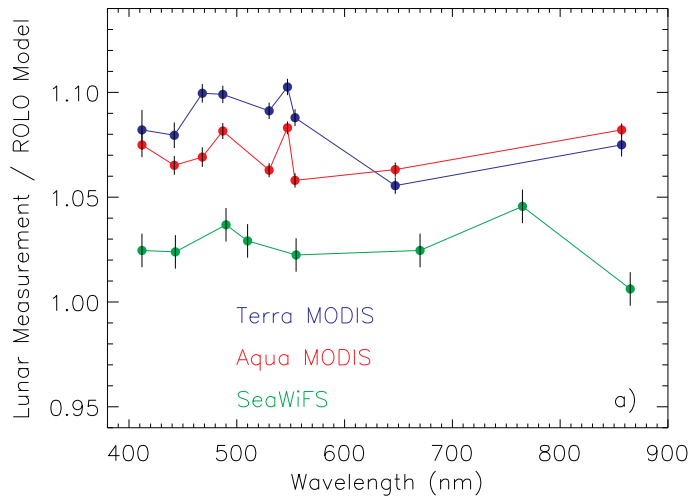
Fig. 6. **SeaWiFS / MODIS Lunar Calibration Comparison.** a) The
three instrument mission-long band averages. b) The SeaWiFS / Terra MODIS
EOS Lunar Calibration Experiment. c) The SeaWiFS / Terra MODIS mission-
long averages and Lunar Calibration Experiment. Eplee_LP130056_fig06a.eps,
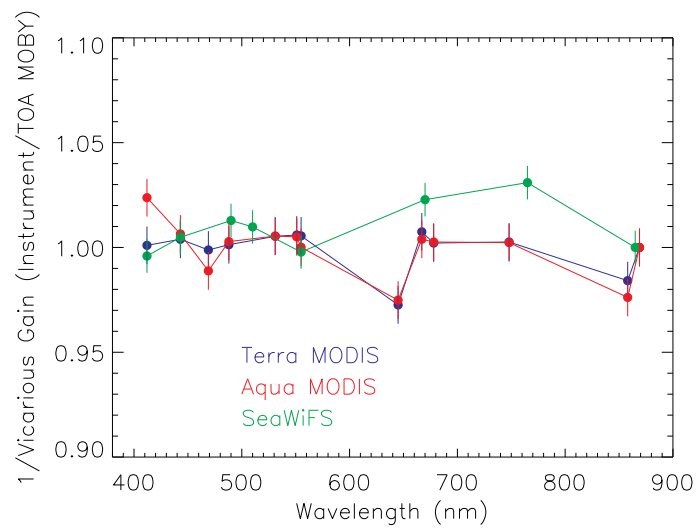Eplee_LP130056_fig06b.eps, Eplee_LP130056_fig06c.eps

Fig. 7. **SeaWiFS / MODIS Vicarious Calibration Comparison.** The inverses of the vicarious gains are plotted so that the SeaWiFS or MODIS measurement is in the numerator of the ratios, allowing comparisons with the lunar observations. Eplee_LP130056_fig07.eps
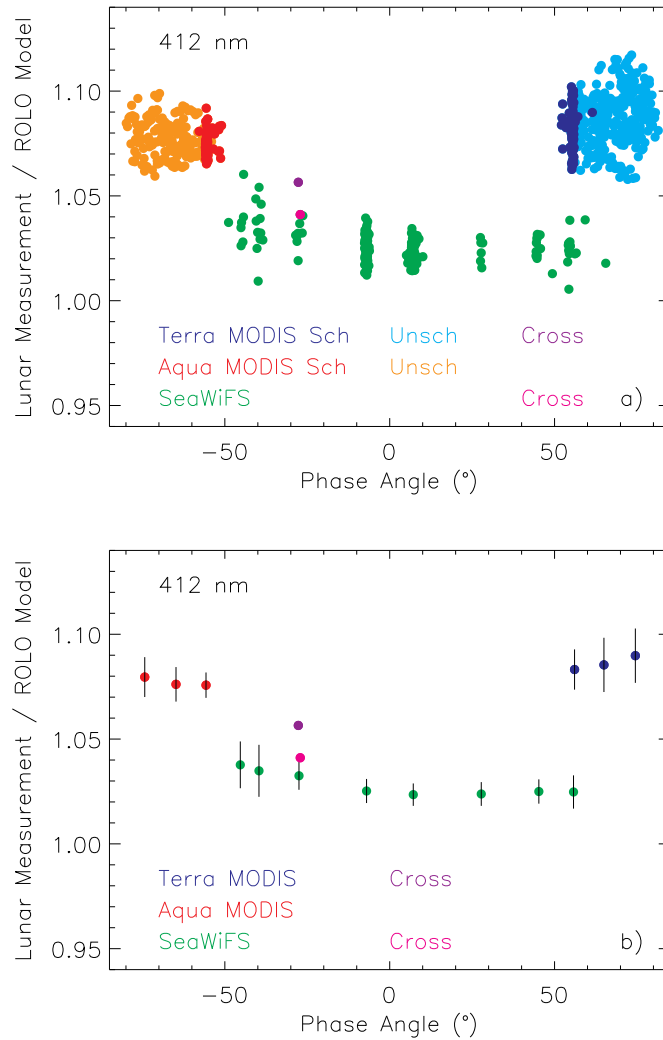
Fig. 8. **SeaWiFS / MODIS Comparison as a Function of Phase Angle.** a) The full lunar data sets are plotted for the 412 nm bands. b) The full data sets are binned and plotted as means with standard deviations for the 412 nm bands. Eplee_LP130056_fig08a.eps, Eplee_LP130056_fig08b.eps